REPORT DOCUMENTATION PAGE

Form Approved
OMB No. 0704-0188

1. REPORT DATE *(DD-MM-YYYY)*	2. REPORT TYPE	3. DATES COVERED *(From – To)*
15 July 2002	Final Report	March 2000 – September 2001

4. TITLE AND SUBTITLE

Acoustic Communication For High-Doppler Guidance and Control

5a. CONTRACT NUMBERS

5b. GRANT NUMBER
N00014-00-1-0357

5c. PROGRAM ELEMENT NUMBER

6. AUTHOR(S)

Lee E. Freitag

5d. PROJECT NUMBER
WHOI 13035700

5e. TASK NUMBER

5f. WORK UNIT NUMBER

7. PERFORMING ORGANIZATION NAME(S) AND ADDRESS(ES)

Applied Ocean and Physics and Engineering Dept.
Woods Hole Oceanographic Institution
86 Water St., MS#18
Woods Hole, MA 02543

8. PERFORMING ORGANIZATION REPORT NUMBER

9. SPONSORING/MONITORING AGENCY NAME(S) AND ADDRESS(ES)

Les Jacobi
Office of Naval Research, Code 333
Ballston Centre Tower One
800 North Quincy Street
Arlington, VA 22217-5660

Eric Garfield
Administrative Contracting Officer
ONR Boston Regional Office
495 Summer Street
Boston, MA 02210-2109

Defense Technical Information Center
8725 John J. Kingman Road
STE 0944
Ft. Belvoir, VA 22060-6218

Naval Research Laboratory
ATTN: CODE 5227
4555 Overlook Avenue SW
Washington, DC 20375-5320

10. SPONSORING/MONITORING ACRONYM(S)
ONR

11. SPONSORING/MONITORING AGENCY REPORT NUMBER

12. DISTRIBUTION/AVAILABILITY STATEMENT

Approved for public release; distribution is unlimited

13. SUPPLEMENTARY NOTES

14. ABSTRACT

See Attached

20020729 103

15. SUBJECT TERMS					
16. SECURITY CLASSIFICATION OF:			17. LIMITATION OF ABSTRACT	18. NUMBER OF PAGES	19a. NAME OF RESPONSIBLE PERSON
a. REPORT	b. ABSTRACT	c. THIS PAGE			Lee E. Freitag
Unclassified	Unclassified	Unclassified	None		19 b. TELEPHONE NUMBER *(Include are code)*
					508-289-3285

Standard Form 298 (Rev. 8-98)
Prescribed by ANSI-Std. Z39-18

Acoustic Communication for High-Doppler Guidance and Control
Final Report

Lee E. Freitag
Woods Hole Oceanographic Institution
266 Woods Hole Road, Mail Stop 18
Woods Hole, MA 02543
Phone: 508-289-3285. Fax: 508-457-2195
lfreitag@whoi.edu

Award: N00014-00-1-0357

TECHNICAL OBJECTIVE

The long-term goal of this program is to provide an acoustic communications system suitable for multiple fast-moving platforms to support the guidance and control function of current and future weapons (Figure 1). The technological objective is the development and testing of single and multi-user acoustic communications solutions suitable for use on weapons systems. The advantage of an acoustic link is that it does not rely upon the wire which is currently used. The wire may break (either accidentally or on purpose) and it restricts the motion of the launching platform. The acoustic link allows multiple platforms to provide the weapon with information, and also allows weapons to communicate in order to coordinate salvo attacks.

TECHNICAL APPROACH

The proposed technology takes advantage of recent work performed as part of the Acoustic Communications ATD which has developed a high-performance acoustic modem for the 688-class SSN. The installation of this capability provides the SSN with a communication system ready to use in controlling off-board vehicles such as torpedoes, provided a means can be found to install similar technology on the weapons. While the initial goal is to utilize the sonar array aboard the existing generation of weapons as the receiver, the work will also focus on optimal usage of next-generation arrays being developed for future systems.

In order to incorporate multi-user access and provide high-reliability while minimizing peak emitted acoustic power the signals will have to be spread in both frequency and time. As a result, the anticipated data rates may be quite low depending on external factors such as desired range and maximum source level. However, in order to accommodate these factors we have developed a scalable methodology for modifying the throughput of the link while maintaining the broadband, multi-access nature of the signals. Acoustic communications tests performed with the high-frequency sail array (HFSP) system have demonstrated 10,000 bps (single-user, no spreading) all the way down to 40 bps (highly spread, low peak power).

Direct-sequence spread spectrum (DSSS) provides two important advantages for underwater communications, it allows the peak signal level to be reduced, though at the expense of bandwidth, and two, it allows multiple users to be accommodated in the same band simultaneously through use of orthogonal codes. The conventional spread-spectrum receiver uses the desired user's code to de-

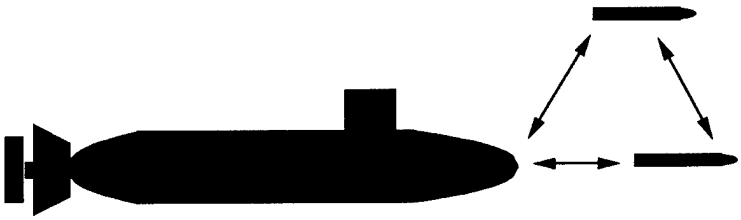

Fig. 1 Proposed operational scenario for platform-weapon communications.

correlate the received signal. The transmitted bit is determined by examining the sign at the output of the de-spreader. While this receiver is used for many terrestrial radio applications, its capability in handling a large number of users is limited due to the residual correlation between different users' codes which is exacerbated by differences in user power levels. There are a number of additional issues as well. In an underwater channel with even small amounts of source-receiver motion the phase of the received signal will vary with time. This phase variation must be tracked in order to successfully recover the data. While in many applications this is done using a pilot tone, CW signals are easy to detect underwater and are not desirable for most applications. Thus the simplest DSSS receiver useful for an acoustic link must also include a phase tracking loop. In addition to rapid phase changes, time-varying multipath present serious limitations to system performance. In particular, the spreading code must be longer than the multipath delay in order to avoid inter-symbol interference. However, to achieve the spreading code gain, the channel must be stationary over the period of the code. In a non-stationary environment, the longer the code, the larger the channel variation over the bit duration, thus reducing the achievable spreading gain. This variation affects the performance of the conventional receiver.

The combination of time-varying multipath, phase motion and Doppler shift all heavily impact the effectiveness of the direct-sequence receiver. In order to increase the usefulness of underwater direct-sequence spread-spectrum systems an adaptive receiver structure [1] which mitigates these effects is proposed. The adaptive front-end reduces multipath and performs Doppler correction [2] at the chip level (before de-spreading). While the receiver introduces additional complexity, it provides a significant increase in performance and allows operation under conditions where direct-sequence spread-spectrum signaling would otherwise be impossible. An equally important feature of the adaptive receiver is its ability to reduce interference from other users [3]. The filter taps are adapted using a minimum mean-square error criterion, which in the presence of interfering users converges to a solution which nulls them to the extent possible using a linear filter. When multiple hydrophones are available the receiver provides MMSE combining to focus on the user of interest through adaptation of the feed-forward filters.

RESULTS

A. Analysis of previously collected high-Doppler data

During a test performed with a static receiver and a fast-moving transmitter, phase-coherent acoustic communication data was collected at up to 10 m/s (about 20 kt). However, an important area of interest to this program is the performance of acoustic receivers at several times this speed. One of the key impacts of fast relative source-receiver speeds is that the apparent rate of channel change increases. In order to study the performance impact in isolation from other effects, the receiver update rate can be

modified to simulate what happens when the platform moves faster through an inhomogeneous ocean. This analysis is valid when it is assumed that the time-expansion or compression effect is compensated without performance loss as the velocity increases.

Thus to simulate the impact of doubling the speed the number of equalizer filter updates is cut in half and the resulting SNR at the output of the receiver measured. This mimics the actual effect of doubling platform motion between two points by removing an intermediate sample point. In effect this doubles the apparent Doppler spread (the spectrum of the complex-valued temporal channel response). The result of performing this analysis for two different types of multipath is shown in Figure 2. The simple multipath case has just one dominant arrival, while the complex case has a spread of over 15 msec which requires more than 100 fractionally-spaced filter taps per hydrophone. The data was originally collected at 7 and 10 m/s respectively, so that the extrapolation at 2-10 times the base rate results in very high simulated speeds.

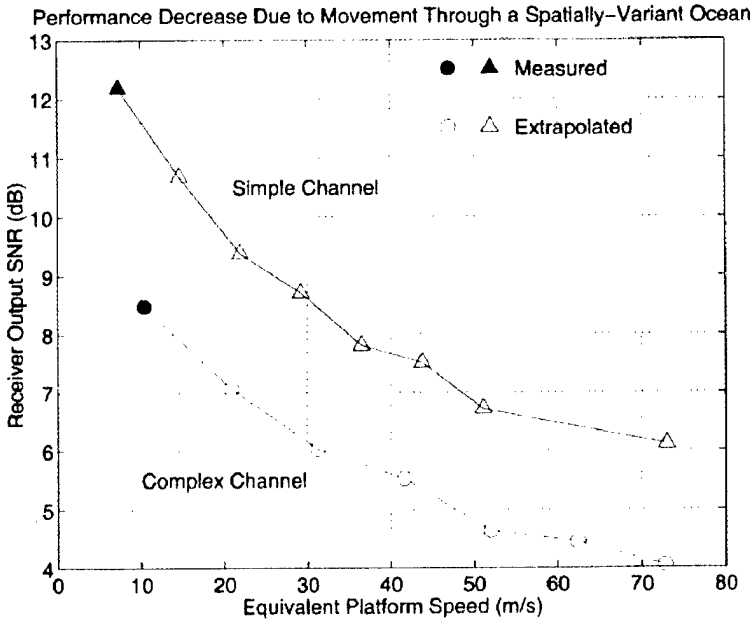

Fig. 2

The result of the decrease in update rate (which simulates faster motion) is that the SNR at the output of the receiver is gradually reduced, which in turn reduces system throughput (or equivalently, increases error rate). The conclusion is that there is no hard boundary where the system stops working, but instead a slow loss in performance results. The multi-rate receiver developed for use with block-coded and spread-spectrum signals can operate through a wide range of output SNR (down to near 0 dB per symbol with high spreading rates) and is thus well-suited to handle this application.

B. In-water Testing with ADCAP Array

Testing with an ADCAP array was conducted with NUWC, Newport in Sept. 2000 to gather acoustic communications data for additional analysis. NUWC performed all work associated with the receiver and WHOI provided the transmitter system including a small boat outfitted with a hydrodynamic source mount which allowed speeds up to 10 knots to be tested. The test was conducted in the North

Test Area of the Narragansett Bay Shallow Water Test Facility. The ADCAP array was deployed using a platform which is lowered into the water from a tower at Gould Island. The facility is part of an extensive torpedo test site built during World War II. Of the 52 channels available on the array, 32 are recorded using a VME-based data acquisition system. Six of the channels were available separately and used for near realtime quick-look of data quality and system performance.

The ADCAP array offers very high quality acoustic signal reception and is well-suited for phase-coherent acoustic communication over its horizontal beam width which is essentially hemispherical. During the test data rates of 10,000 bps were demonstrated at ranges up to several kilometers.

Also of interest to this program is the use of the array for multi-user communication using spread-spectrum signals. For example, in a multi-platform battle group situation several data streams of targeting information may be available asynchronously from several sources. As an example of how the receiver works with two users, two spread-spectrum signals from two different users were added together with the amplitude of one user set to four times the other. One channel of the summed signal is shown in Figure 3a. In this case 5 array channels were used by the multi-channel receiver which achieved the results shown in Figure 3b. The amplitude of a perfectly de-spread signal (with perfect equalization and Doppler compensation) would be 63 (the spreading code length). When only user 1 is present the result is indeed very near this value and the SNR of the data symbols is almost 20 dB. When the second user starts there is a visible impact, but the SNR is still greater than 11 dB, which provides for very reliable (low error-rate) communication.

C. Development and Analysis of Integrated Doppler Tracking and Adaptive Equalization.

As a part of this program we have also completely documented the performance of the Decision Feedback Equalizer with integrated Doppler shift acquisition and tracking. This work is described in the draft paper submitted to the IEEE Journal of Oceanic Engineering entitled "Integrated Dopper Tracking and Interpolation for Phase-Coherent Acoustic Communication" and attached as an appendix to this report. The work includes the following major sections:

- Introduction with both motivation and a review of the literature for relevant previous publications.
- A simple channel model which describes the effect of source-receiver velocity on the baseband communications signal and defines variables for frequency shift, time-scaling and Doppler spread.
- An introduction to the problem of time-varying interpolation and the derivation of an efficient method for real-time compensation of the time-scale change of a Doppler-shifted signal. The method includes a simple adjustment for the quality of the interpolation process so that it may be matched to a particular SNR or signal constellation density.
- Detailed receiver description including the equalizer, phase-locked loop and interpolation.
- Results of using the receiver algorithm in four different test cases, one of which includes over one hundred data packets.

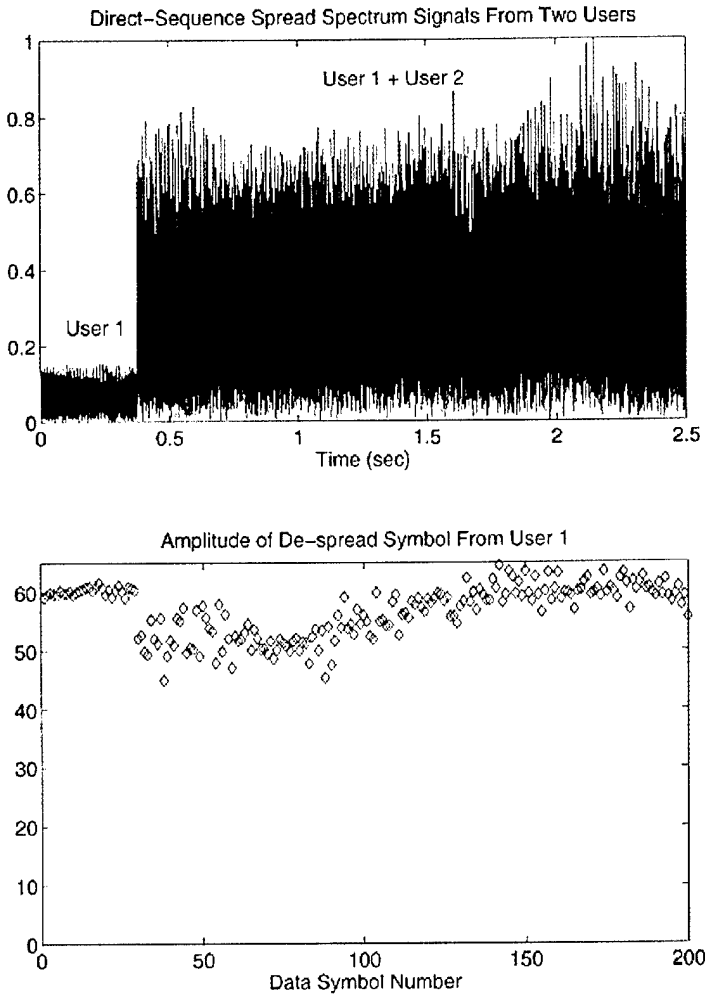

Figure 3 (a) Two users summed together with user 2 four times user 1. (b) Decoded data from user 1 showing a small impact when user 2 starts transmitting.

RELATED PROJECTS

"Acoustic Communication System Development and Analysis", This work is performed at WHOI and it is funded by ASTO (Program Manager: Tam Nguyen). This is a follow-on to the ACOMMS ATD. Work on this program includes the HF SSN acoustic communication system, which the weapon-based system is intended to communicate with.

REFERENCES

[1] Stojanovic, M., J. Catipovic and J. Proakis, "Phase coherent digital communications for underwater acoustic channels", IEEE J. Oceanic Eng., Vol. OE-16, pp. 100-111, January 1994.

[2] Johnson, M., L. Freitag and M. Stojanovic, "Improved Doppler tracking and correction for underwater acoustic communication," in Proc. ICASSP'97, Vol. 1, pp. 575-578, Munich, Germany, April, 1997.

[3] Glisic, S. and B. Vucetic, Spread-Spectrum CDMA Systems for Wireless Communication, Boston: Artech House, 1997.

Note: See also the reference list in the attached paper.

Integrated Doppler Tracking and Interpolation for Phase-Coherent Acoustic Communication

Lee Freitag, Mark Johnson and Milica Stojanovic

M. Johnson and L. Freitag are with the Woods Hole Oceanographic Institution, Woods Hole, MA. M. Stojanovic is with the Massachusetts Institute of Technology, Cambridge, MA.

Abstract

A computationally efficient method for integrating Doppler frequency shift estimation and sample rate interpolation of an acoustic communication signal in a time-varying environment is proposed. The estimation of the Doppler shift is performed using a second-order phase-locked loop in conjunction with the decision-feedback equalizer. Initial acquisition is accomplished during the training period of the equalizer so that a separate estimation step is not required. Tracking of the Doppler shift continues in decision-directed mode. Interpolation based on the Doppler estimate is performed using a filter bank which is optimized in the least-squares sense for fractionally-spaced sampling. The total computational requirement is proportional to the length of the interpolation filters and the update rate of the interpolator, which is made efficient through the use of a pre-computed filter bank. The length of the filters is determined by the SNR required to support a given constellation density and simulation results are presented to demonstrate the performance of the interpolator. Results from in-water testing show the performance advantage of continuous Doppler tracking in a time-varying environment. Test environments include both shallow and deep-water, rates of 2500 to 10000 bits per second, and center frequencies of 2 to 25 kHz. The capability of the method to track Doppler through multiple sign changes is demonstrated with a 60 second long transmission from a vessel traveling in a circle at 2 m/s.

Keywords

Doppler shift, acoustic communication, PLL, interpolation, timing recovery, symbol synchronization, filter bank, underwater vehicles.

I. INTRODUCTION

Relative motion between a source and receiver causes both a frequency-shift and time-scale change in a communication signal. The distortion due to the Doppler shift is proportional to the ratio of propagation speed to relative platform speed. In the underwater acoustic channel the propagation speed is low relative to potential source-receiver velocities, leading to time-scale changes which are significantly greater than those encountered at radio frequencies. Time compression or expansion of 0.1% is typical for slow-moving systems, but can reach 1% when two fast-moving underwater vehicles attempt to communicate. The effects vary with time when relative accelerations due to speed or course changes are present. When both source and receiver are in motion, the resulting acceleration may exceed $1\ \mathrm{m/s^2}$. An example of a high acceleration platform is a wave-following buoy. At sea-state 6 the vertical acceleration of a wave-following buoy may reach $4\ \mathrm{m/s^2}$, requiring fast sample rate adaptation. The effects of large time-scale changes will adversely affect the throughput of high-rate, bandwidth-efficient communication unless tracked and removed.

The fractionally-spaced decision feedback equalizer (DFE) adapted using the minimum mean-square error (MSE) criterion will adjust the feedforward filter coefficients to compensate for both carrier phase offset and sample-rate error [1]. However, as pointed out in [2], relying on the equalizer to correct for carrier phase shift results in excess MSE because the tracking gain must be set higher than if the phase shift were compensated using an explicit tracking loop. While the MSE-adapted filter is capable of performing time-scale interpolation as well, there are several reasons to consider a separate interpolator. The first reason is the same as that which motivates separate carrier phase recovery: an equalizer with tracking rate optimized for ISI removal, phase recovery *and* time-scale interpolation will operate with a higher MSE than an equalizer only tracking ISI. In addition, when interpolation is performed by the equalizer, the reference tap will eventually move out of the filter window as the symbol timing error slowly grows. While this can be alleviated through the use of filter lengths sufficient to span the maximum time compression or expansion, excess MSE and reduced tracking capability may result from the use of needlessly large filters.

The phase tracking technique presented here stems from PLL design and analysis work in [3] which were incorporated into the single-channel [4] and multi-channel [5] DFE for use in the underwater environment. These receivers were subsequently modified in [6] to improve tracking performance and in [7] to use a single tracking loop for a multi-channel receiver with long feed-forward filters. This phase tracking method forms the starting point for the Doppler estimation portion of the receiver described here.

Optimal digital interpolation for band-limited signals is discussed in [8] and [9]. Additional work presented in [10] and [11] provides background on interpolation methods focused on sample-clock recovery. While the underwater application differs from than that in [9] or [11], the analysis of interpolator performance for an over-sampled signal is relevant to the design of baseband digital interpolators for the Doppler-compensation problem.

Several Doppler compensation methods focused on underwater acoustic communication have been proposed. In [6] a method for estimating the Doppler shift at the start of a data packet and then interpolating the entire packet at the same rate was presented. For constant Doppler this technique performs well and offers identical performance to that proposed here. Another fixed-estimate approach was reported in [12]. This method measures the time delay between

dedicated signals inserted into the data stream and uses the measured temporal expansion or contraction to calculate the interpolation rate. The interpolation is then performed on the block of data between the two measured signals.

A method for estimating the time-varying Doppler of m-sequences used for tomography [13] treats topics similar to those presented here, but the need to operate at a very low symbol SNR leads the authors to develop a heterodyning and low-pass filter approach which differs significantly from the proposed decision-directed approach.

The contribution of this paper is an efficient time-varying Doppler compensation method which operates at the baseband sampling rate and offers low latency. The proposed method is thus suitable for real-time implementation using inexpensive digital signal processors with limited memory. For typical autonomous vehicle speeds of 1-3 m/s, the DFE training data is used to acquire the Doppler shift, which is then tracked in decision-directed mode for any packet length. No additional timing recovery sequences are required and high-rate Doppler tracking is achieved independent of packet length. When the expected Doppler is high, an additional estimation step may be used to provide an initial starting point for the integrated tracking system.

Through variation of the filter-bank size and filter update rate the residual error of the interpolator can be modified to suit the SNR of any PSK or QAM constellation. Thus the computational load is optimized to meet an actual fidelity requirement.

The paper is organized as follows: in Section II the model of the Doppler-shifted communication channel is presented. Section III presents the interpolation filter design method and summarizes its performance. In Section IV, the PLL, DFE and sample-rate estimation process is discussed. Results of in-water testing are included in Section V.

II. Channel Model

The shallow water channel is modeled by a time-varying impulse response

$$c(\tau, t) = \sum_{p=1}^{P} c_p(t)\delta(\tau - \tau_p(t)) \tag{1}$$

where t denotes the time of observation, and τ denotes the delay. Two phenomena characterize this channel: time spreading and frequency spreading. Time spreading is caused by propagation over multiple paths, distinguished by indices p in the above model. In shallow water, multipath propagation is mainly caused by signal reflections from the surface, bottom and any objects in

the water. Reflections that reach the receiver with significant energy determine the total number of paths P needed to represent the channel response. Each path is described by a gain $c_p(t)$ and a delay $\tau_p(t)$. Frequency spreading is caused by the time-variability of these quantities.

For low relative source-receiver speeds, time-variation of the path delays is often neglected. This approximation is justified when signals are transmitted in short packets such that no significant changes in path delays occur over the packet. Consequently, it suffices to design a receiver as if the path delays were constant. The maximum path delay then represents the multipath spread of the channel and serves to determine the size of equalizer filters needed for digital interpolation prior to adaptive equalization. Any frequency spreading in this case is caused by the time-variation of the path gains only. An adaptive equalizer will track this time-variation provided that it is slow relative to the data rate. For time-varying channels the rate of time-variation is represented by the Doppler frequency spread.

Path gains are often modeled as random processes, and described by the second-order statistics:

$$R_p(\Delta t) = E\{c_p(t + \Delta t)c_p^*(t)\}. \tag{2}$$

The Fourier transform of the above autocorrelation function is termed the Doppler power spectrum of the random process $c_p(t)$:

$$S_p(\nu) = \int_{-\infty}^{+\infty} R_p(\Delta t)e^{-j2\pi\nu\Delta t}d\Delta t. \tag{3}$$

The bandwidth of this function is the Doppler spread which quantifies the frequency spreading of the signal traveling on the pth path. The shape of the Doppler spectrum depends on the model used to represent the randomly time-varying path gains. To compensate for the time-varying inter-symbol interference caused by the time-varying multipath processes $c_p(t)$, the receiver employs an adaptive equalizer.

In mobile underwater communication systems, explicit motion between the transmitter and receiver introduces additional time-variation of the channel. This time-variation becomes a dominant factor in determining the frequency spreading properties of the channel when mobile units are moving at speeds of several m/s. At such speeds, changes in the propagation path length that occur in one data packet cannot be neglected. Time-variability of the path delay causes dilation or compression of the signal in time which must be taken into account when designing a receiver.

A simple model for the time-dependence of path delay can be obtained by considering receiver-transmitter motion at a constant relative speed v. The resulting Doppler spread will be a function of the speed v normalized by the speed of sound c. The exact relation depends to the statistical model of the entire scattering process. Nevertheless, it is possible to develop a simplified model, without any statistical assumptions, to provide at least an insight into the Doppler spreading process caused by the receiver/transmitter motion. To do so, let us consider transmission of a signal $s(t)$, which represents a baseband signal $u(t)$ modulated onto a carrier of frequency $f_c = \omega_c/2\pi$

$$s(t) = Re\{u(t)e^{j\omega_c t}\}. \tag{4}$$

Relative motion between the transmitter and receiver results in the variation of the path length traveled by the signal. Let us consider a single propagation path, and let the distance between the transmitter and the receiver at time t_0 be l_0. The signal received at time t is then:

$$r(t_0) = s(t_0 - l_0/c). \tag{5}$$

At a subsequent time instant, $t_0 + \Delta t$, the receiver has moved away from the transmitter so that the distance between them is now $l_0 + l$. Since the relative speed of this motion is v, the distance traversed during Δt is $l = v\Delta t$. (There is no loss of generality in assuming a different direction of the motion.) Hence, the signal received at time t_0+t is equal to the signal transmitted $(l_0+l)/c$ seconds earlier:

$$r(t_0 + \Delta t) = s(t_0 + \Delta t - (l_0 + v\Delta t)/c) \tag{6}$$

Setting $t_0 + \Delta t = t$, the received signal can be expressed in terms of a time-varying delay $\tau(t)$ as

$$r(t) = s(t - \tau(t)) \tag{7}$$

where

$$\tau(t) = \tau_0 + vt/c \tag{8}$$

$$\tau_0 = l_0/c - vt_0/c \tag{9}$$

Alternatively, the received signal can be expressed as

$$r(t) = s(at - \tau_0) \tag{10}$$

where

$$a = 1 - v/c \tag{11}$$

is the time-scaling factor. The scale factor is less than 1 when v is positive (range opening, time expansion).

To distinguish the effects of Doppler spreading and Doppler shifting, it is insightful to look at the equivalent baseband representation of the received signal:

$$r(t) = Re\{v(t)e^{j\omega_c t}\}. \tag{12}$$

Upon substituting for the signal $s(t)$ in terms of its baseband equivalent $u(t)$ in the expressions for the received signal $r(t)$, it is found that

$$v(t) = u(at - \tau_0)e^{j\phi_0}e^{j2\pi f_{dv}t} \tag{13}$$

where $\phi_0 = \omega_c\tau_0$ is the constant phase offset, and $f_{dv} = -f_c v/c$ is the Doppler shift. The carrier frequency thus appears shifted at the receiver by the amount $f_{dv} = \omega_{dv}/2\pi$. The Doppler spread is caused by time-scaling, as described by the factor $a \neq 1$. The frequency occupancy of the received signal is evident from the Fourier transform of the baseband equivalent $v(t)$:

$$V(f) \sim U((f - f_{dv})/a). \tag{14}$$

Thus, the transmitted baseband signal of bandwidth B centered around 0 Hz is observed at the receiver (after nominal carrier demodulation) as a signal of bandwidth aB (Doppler spreading) centered around f_{dv} Hz (Doppler shifting).

Motion-induced Doppler spreading and shifting are hence both characterized by the factor v/c. Unlike in the case of radio communications, where this factor is at most on the order of 10^{-7} (for a vehicle speed of 100 km/h), in an underwater acoustic scenario it is on the order of 10^{-2} for vehicle speeds of about 5 m/s. As a consequence, the time-scaling effect is not negligible in an underwater mobile system. It should be noted that in a realistic scenario, the relative speed v will be varying in time. Consequently, the Doppler spread calculated above can only be regarded as an instantaneous value, i.e. as one among a range of values that the true spreading (and shifting) will be assuming in time. Also, depending upon the geometry of the channel, different propagation paths will experience different frequency spreading. The

magnitude of this problem necessitates use of explicit phase and delay tracking to aid in the operation of an adaptive equalizer in the mobile underwater channel.

III. Efficient Time-Varying Interpolation

The fractional sampling-rate deviation caused by Doppler shift is difficult to correct using the conventional re-sampling technique, i.e., interpolation by an integer factor M, followed by decimation by another factor, N. This method adjusts the input sampling rate by a factor M/N. Thus to achieve a small sampling-rate change, N and M must be large (e.g., for a -0.5% change equivalent to a relative speed of 7.5 m/s, M and N would be 199 and 200, respectively). A computationally expensive filtering operation is required at the high intermediate sampling rate, Mf_b, where f_b is the baseband sampling rate, making this method impractical.

An alternative approach is to interpolate the input signal using a time-varying FIR filter. For a fractional sampling rate variation of $\delta = v/c$ (which may be time-varying), the output samples from the interpolator are, ideally: y_k, $y_{k+1+\delta}$, $y_{k+2+2\delta}$,..., where y_k, y_{k+1},... are the input samples and the fractional index $n\delta$ implies interpolation between the neighboring points in y_k. The output samples are approximated through interpolating successively by $\delta, 2\delta, 3\delta, \ldots$ on a sliding window of the input signal. The computational cost of this method is proportional to the baseband sampling rate time the filter length plus the cost of generating the interpolation filter for each output sample. Interpolating filters can be computed iteratively, or selected from a look-up-table. Iterative computation has the advantage of producing a specific filter giving the exact phase lag required, but is restricted by complexity considerations to short interpolation filters which may introduce spectral distortion and noise. The look-up-table method allows the use of longer filters but requires an approximation in phase lag due to the limited number of filters to choose from.

A method which combines the advantages of each of these approaches has been developed to reduce computational effort and memory usage while minimizing spectral distortion in the signal band. The algorithm includes a method for computing optimal interpolating filter tables and a fast method for interpolating between filters in the look-up table to permit the use of a small filter bank. In addition, the effect of updating the filters at a rate less than the symbol rate is examined as a means of reducing computations.

A. Time-Delay Filter Design

There are two key components in the interpolator. The first is an accumulator used to determine the fractional time delay $\tau(i) = \tau(i-1) + \delta(i)$ required for the next output sample. The second component in the interpolator is an algorithm for computing filter coefficients for a given time delay. This algorithm produces filters which are selected to provide a satisfactory trade-off between computational burden and interpolator error (i.e., noise due to spectral distortion by the filter).

In a coherent acoustic communications receiver, a fractionally-spaced equalizer is often used to compensate for the lack of optimal timing. For the input sampling rate of $f_b = 2/T$ Hz where the signal energy is constrained to $\pm 1/T$ Hz, it is only necessary for the interpolator to provide accurate Doppler correction at frequencies up to half the symbol-rate. This suggests that a frequency-weighted approach to time-delay filter design can be used to achieve optimal performance from short, computationally-efficient filters.

The ideal frequency response of a time-delay filter is $D(e^{j\omega}) = e^{-j\tau\omega}$, where τ is the filter time delay in fractions of a sample. As noted above, this need only be maintained accurately over the frequency range $-\omega_0 < \omega < \omega_0$, where ω_0 is the upper frequency limit of the signal of interest in radians per second. The bandlimited mean-square-error between the desired and actual filter responses is defined as

$$\gamma = \int_{-\omega_0}^{\omega_0} |D(e^{j\omega}) - H(e^{j\omega})|^2 d\omega \tag{15}$$

where $H(e^{j\omega})$ is the frequency response of the candidate filter. Using an FIR filter realization with N samples of causal support yields a time-delay filter with $P = 2N + 1$ values. The filter coefficient vector $\mathbf{h} = [h_{-N}, \ldots, h_0, \ldots, h_N]^T$ so that $H(e^{j\omega}) = \mathbf{h}^T W$, where $W = [e^{-jN\omega}, \ldots, 1, \ldots, e^{jN\omega}]^T$. The filter coefficients that minimize γ can be determined by differentiating (15) with respect to $\mathbf{h}$ and setting the derivative to 0:

$$\frac{d\gamma}{d\mathbf{h}} = \int_{-\omega_0}^{\omega_0} \{2WW^H\mathbf{h} - 2\mathrm{Re}(e^{j\tau\omega}W)\} d\omega \tag{16}$$

where W^H denotes the conjugate transpose. Setting the result to 0 yields

$$\mathbf{h} = \left(\int_{-\omega_0}^{\omega_0} WW^H d\omega\right)^{-1} \mathrm{Re}\left(\int_{-\omega_0}^{\omega_0} e^{j\tau\omega} W d\omega\right). \tag{17}$$

Defining

$$\mathbf{R} = \int_{-\omega_0}^{\omega_0} WW^H d\omega \tag{18}$$

and

$$\mathbf{p} = \mathrm{Re}\left\{\int_{-\omega_0}^{\omega_0} e^{j\tau\omega} W d\omega\right\} \tag{19}$$

(17) becomes the familiar least-squares solution

$$\mathbf{h} = \mathbf{R}^{-1}\mathbf{p} \tag{20}$$

where

$$\mathbf{R} = 2\begin{bmatrix} \omega_0 & \sin\omega_0 & \frac{1}{2}\sin 2\omega_0 & \cdots \\ \sin\omega_0 & \omega_0 & \sin\omega_0 & \cdots \\ \frac{1}{2}\sin 2\omega_0 & \sin\omega_0 & \omega_0 & \cdots \\ \vdots & \vdots & \vdots & \ddots \end{bmatrix} \tag{21}$$

and

$$\mathbf{p} = 2\begin{bmatrix} \frac{\sin(\tau-n)\omega_0}{\tau-n} \\ \vdots \\ \frac{\sin\tau\omega_0}{\tau} \\ \vdots \\ \frac{\sin(\tau+n)\omega_0}{\tau+n} \end{bmatrix}. \tag{22}$$

Only $\mathbf{p}$ is dependent on the time delay, τ, and so for a given filter length, only one matrix inversion is necessary to compute the entire filter bank.

For the full-band case ($\omega_0 = \pi$), $\mathbf{R} = 2\pi\mathbf{I}$ and $\mathbf{p} = [\mathrm{sinc}(\tau-n), \ldots, \mathrm{sinc}(\tau), \ldots \mathrm{sinc}(\tau+n)]^T$, where $\mathrm{sinc}(x) = \sin(\pi x)/\pi x$. In this case the least-square interpolator is identical to the sinc function interpolator and thus the sinc function interpolator is the optimal full-band interpolator using the criterion in (15).

B. Time-Delay Filter Bank

The least-squares filter computation algorithm corresponding to (20) requires $(2N+1)^2$ operations per filter (assuming that $\mathbf{R}$ is inverted off-line), making it unsuitable for real-time computation. A better strategy is to pre-compute a range of time-delay filters and select the one closest to the required time-delay at each sample. For a given filter bank size, two techniques can be used to improve accuracy.

The first technique exploits the inherent symmetry in the filters to minimize the range of filters needed in the filter bank. This follows from the observations that (i) a negative time delay of τ samples can be realized by reversing the coefficients of a positive τ time-delay filter, and (ii) a time-delay > 0.5 can be realized by a unit-sample shift and a negative time-delay filter of $\tau - 1$ samples. Exploiting these facts, it is only necessary to have time delays between 0 and 0.5 samples represented in the filter bank.

The second technique for improving accuracy is to interpolate between filters in the filter bank. Using first-order interpolation the time-delay filter for a desired delay τ is approximated as

$$\mathbf{h}(\tau) = \mathbf{h}(\tau_0) + \frac{\tau - \tau_0}{\tau_1 - \tau_0}(\mathbf{h}(\tau_1) - \mathbf{h}(\tau_0)) \qquad \tau \in [\tau_0, \tau_1] \tag{23}$$

where τ_0 and τ_1 are the two flanking time delays represented in the filter bank. The computation burden of (23) can be reduced at the expense of memory by pre-computing the scaled difference filter bank:

$$\mathbf{g}(\tau_i) = \frac{1}{\tau_{i+1} - \tau_i}(\mathbf{h}(\tau_{i+1}) - \mathbf{h}(\tau_i)) \tag{24}$$

for $i = 0, \ldots, 2N + 1$. Using (24), (23) simplifies to

$$\mathbf{h}(\tau) = \mathbf{h}(\tau_0) + (\tau - \tau_0)\mathbf{g}(t_0). \tag{25}$$

To summarize, for an M-filter bank at a time delay of τ samples:

1. Subtract or add 1 to τ until $-0.5 < \tau < 0.5$. Shift the filter window right (left) for each subtraction (addition).
2. Find the closest time delay to $|\tau|$ represented in the filter bank.
3. Interpolate using (25) ($2N + 1$ operations).
4. Reverse the filter if τ is negative.

C. Filter Update Rate

Depending on the magnitude of the Doppler shift and the symbol rate, the filter may not need to be updated for each output sample. The same filter can be used for a number of samples with only a small increase in noise when the sample rate adjustment is on the order of 0.25% ($v =$ 3 m/s). This significantly reduces the number of computations needed for the filter selection portion of the interpolation process.

The performance of the interpolator for filters of 3 to 15 taps and update periods from 2 to 60 samples is shown in Fig. 1. The frequency weighting is set to 0.5 of Nyquist (i.e. $\omega_0 = \pi/2$) and the interpolation rate is 1.0025. The noise level is computed by measuring the difference between the interpolator output and the ideal output for a sine wave input at each frequency and then integrating this noise over the communication band.

The filter length and update period for a given density constellation can be selected based on Fig. 1. BPSK and QPSK modulation require only low SNR and so can tolerate short filters and infrequent updates, while 16-QAM requires a 9-15 length filter with frequent updating. Thus the computational requirements of the interpolation subsystem can be matched to a particular PSK or QAM constellation.

IV. The Receiver

The complete receiver, excluding the front-end demodulator, is shown in block diagram form in Fig. 2. The receiver embodies a multi-channel decision feedback equalizer (DFE) with 2nd order phase-locked loop (PLL) [4] and the time-varying interpolator described in Section III. While the receiver described in [4] employs one PLL per input channel, here a phase estimate $\hat{\theta}(i)$ from a single PLL, is applied to the composite symbol estimate from all channels [7].

For ease of explanation a $1/T$-rate single-channel version of the DFE will be considered. Extensions to the fractionally-spaced multi-channel case follow from [4] and [6]. Let the complex baseband received signal be represented by $y(i)$ and let the current estimate of the sample-rate error be $\delta(i) = v(i)/c$, where $v(i)$ is the current relative speed between source and receiver.

The sample rate of the discrete signal $y(i)$ is adjusted using the length $P = 2N + 1$ interpolation filter $\mathbf{h}(\tau_i)$ generated using (25). The filter $\mathbf{h}(\tau_i)$ is computed using the cumulative delay in symbols at symbol i given by the recursive equation:

$$\tau(i) = \tau(i-1) + \delta(i). \tag{26}$$

The ith time-scale corrected symbol is then computed by applying the current interpolation filter to

$$x(i) = \sum_{k=1}^{P} H_i(k) y(i + m - N + k - 1)$$

where m is the positive or negative integer portion of $\tau(i)$ which shifts the interpolating filter window to track the change in time scale. The interpolated signal $x(i)$, together with the previous hard decisions $\tilde{d}$ and the phase estimate $\hat{\theta}(i)$ from the PLL are used to update the equalizer and compute the current symbol estimate

$$\hat{d}(i) = \Phi^H(i)\Theta(i)e^{-j\hat{\theta}(i)}$$

where $\Phi(i) = [x(i), x(i-1), \ldots, x(i-N_f-1), \tilde{d}(i-1), \ldots, \tilde{d}(i-N_b)]$, N_f is the number of feedforward taps and N_b is the number of feedback taps.

The feedforward and feedback filter coefficients in $\Theta(i)$ are jointly-updated using an algorithm from the RLS or LMS families [7] and the symbol error is computed using

$$e(i) = \tilde{d}(i) - \hat{d}(i),$$

where $\tilde{d}$ is the hard decision associated with the current symbol estimate. The phase estimate $\hat{\theta}(i)$ is computed as shown in [4] or [6], then low-pass filtered prior to use in updating the time-shift $\tau(i)$.

First, the instantaneous Doppler shift frequency f_{dv} is estimated from the slope of the low-pass filtered phase estimate $\theta'(i)$:

$$f_{dv}(i) = \frac{1}{2\pi T}(\theta'(i) - \theta'(i-1)).$$

The fractional Doppler shift factor $\delta(i) = v(i)/c$ is then computed using the carrier frequency f_c:

$$\delta(i) = v(i)/c = f_{dv}(i)/f_c.$$

This value is used in (26) to complete the interpolating loop in the receiver.

The operation of the equalizer is as described in [4], with the exception that the PLL is also used to estimate the Doppler shift frequency and from it the new sampling rate via the outer feedback loop. During the equalizer training period the phase and Doppler shift are acquired simultaneously. While normally $\delta(0)$ is initialized to 0, if an estimate of the Doppler shift at the start of a packet is available (e.g. computed as described in [6]), then $\delta(0)$ may be initialized to this value which will reduce the number of symbols required for acquisition.

The total number of computations required to generate the time-scale estimate is very small. Thus, this approach, when combined with the interpolation filter update method of Section III, provides an extremely efficient way of removing the time-dilation or compression from phase-coherent signals.

V. RESULTS

The receiver described above has been tested in a number of acoustic channels with different data rates and carrier frequencies. Results from these experiments demonstrate the performance improvement due to the new technique, with and without the use of an initial Doppler estimate. Four test cases are discussed here: (A) 1250 symbols per second (sps) QPSK at the carrier frequency 2.25 kHz, (B) 5000 sps 8-PSK at 15 kHz, (C) 5000 sps QPSK at 25 kHz, and (D) 4000 sps BPSK at 15 kHz. Cases A, B and D are single packet performance examples, while case C includes over one hundred packets at a variety of relative speeds and ranges.

A. 1250 sps at 2.25 kHz Carrier, QPSK

The first case is from a test carried out in 1996 on the New England continental shelf in 150 m deep water at 6 km range [16]. This test is of interest because it includes a constant relative speed of 2.2 m/s plus a smaller time-varying component. The channel delay-spread (Fig. 3) is almost 0.1 s and the data is collected on a multi-channel vertical array. Additional details are provided in [16].

To demonstrate the performance difference of interpolating and non-interpolating receivers the data is processed three different ways. The first uses the PLL, but no interpolation at all. In this case the adaptive equalizer adjusts the feedforward taps as best it can in order to correct for the time-scale offset. In the second receiver the Doppler shift is estimated as shown in [6] then phase-shifted and interpolated to correct for the Doppler-induced time scaling prior to equalization. Finally, the complete receiver with integrated Doppler estimation and compensation is used.

The performance of the DFE with PLL only is shown in trace A in Fig. 4. The average MSE is approximately -10 dB, which is sufficient for reliable operation of the DFE. While the PLL-only receiver works in this case, it is unusual for this receiver to operate reliably in decision-directed mode when there is source-receiver motion. The performance of the DFE with PLL operating on the received signal after a constant Doppler is removed by carrier shifting and interpolation is shown in trace B in Fig. 4. The performance improvement is dramatic, on average the MSE is almost 10 dB better than without interpolation.

However, the carrier phase recovered by the PLL after the constant Doppler shift is removed

shows that there are changes in the Doppler that occur during the packet (Fig. 5). The phase contains a small linear trend plus a sinusoidal component. The slope of the phase corresponds to a slight error in the initial estimate (0.2 Hz), while the 1 Hz sinusoidal signal is due to motion of the tow body that the source is mounted on.

The equalizer with integrated interpolation provides additional improvement in MSE by compensating for the change in time scale within the packet. The MSE for the fully integrated receiver is shown in trace C in Fig. 4. The performance difference between the fixed and integrated interpolation receivers depends upon the change in Doppler relative to that estimated at the start of the packet. As shown in Fig. 4 the instantaneous performance difference can be as much as 5 dB between the fixed and integrated receivers, and 15 dB between the fully integrated and non-interpolating receivers.

Finally, it should be noted that in this particular case the performance difference between the integrated Doppler-tracking equalizer with and without an initial Doppler estimate is nearly zero because the overall shift is small, only 3.4 Hz. The PLL acquires this carrier frequency offset during the training period and tracks it at a loop gain that does not introduce excess noise into the equalizer output. In test case C below the performance difference between these two modes is examined in detail.

B. 5000 sps, 15 kHz Carrier, 8-PSK

A deep-water vertical acoustic communication link from a bottom instrument to a ship or buoy experiences Doppler shifts due to platform motion induced by surface waves. Even moderate sea-states may generate vertical speeds of 1 m/s, depending upon the response of the platform. A test conducted in 3000 m water using 5000 sps 8-PSK modulation (15000 bps) demonstrates the fast rate of change due to surface wave motion. In Fig. 6 the phase recovered by the PLL is shown along with the corresponding time scale change. In this test case the interpolation rate changes quickly and constantly throughout the 1.4 s packet, with a maximum sample-rate change of 0.11%. The receiver with continuously estimated Doppler shows a 3 dB improvement over the receiver that uses a single estimate of Doppler made at the start of the packet.

This example illustrates another important aspect of the interpolator: maintaining the reference tap of the equalizer so that the feedforward filter is aligned in time with the signal. This movement is illustrated in Fig. 7 (top), where the feedforward tap weights adapt to follow the

time-scale change in the uncompensated case. This packet is relatively short and the feedforward filters are wide, so that by the end of the packet τ is still less than the feedforward filter width. Time-varying interpolation adjusts the reference point of the equalizer to track the delay and maintain symbol synchronization (bottom of Fig. 7). This has the additional benefit of requiring the feedforward filters to span only the channel delay spread, in this case 6 taps. In the uncompensated case 20 taps are necessary, increasing the computational requirement and slowing the adaptation rate.

C. 5000 sps at 25 kHz Carrier, QPSK

To demonstrate the performance of the equalizer with both fixed and adaptive interpolation over a wide range of operating conditions the receiver was tested on a large data set where both the Doppler and the propagation channel vary. The track of the source and receiver are shown in Fig. 8, and the relative velocity and range between source and receiver are shown in Fig. 9. This test was performed in water approximately 150-200 m deep on the New England Continental Shelf. The data packets are about 7500 symbols long (1.5 s).

The signals recorded during this test show a wide range of characteristics due to the variety of maneuvers performed by the source vessel. In some packets the Doppler (whether low or high) is constant throughout, while in other packets the Doppler varies significantly from the initial estimate. The performance improvement of the integrated interpolation technique depends upon the Doppler change and whether or not an initial Doppler estimate is used. When an initial Doppler estimate is used the required phase-locked loop gain is lower and the error due to tracking lag is reduced.

Each data packet is in processed three different ways: (a) using an initial Doppler estimate but without continuous tracking, (b) using the initial estimate plus continuous tracking, and (c) acquisition of the initial Doppler shift during training then continuous tracking. The results are summarized in Fig. 10 where the difference in SNR at the output of the equalizer for the receivers with integrated interpolation are plotted with respect to the receiver using interpolation based on a single Doppler estimate made at the start of the packet.

The interpolating receiver initialized with an externally-obtained Doppler estimate produces the best overall performance when the relative source-receiver speed is high. As shown in Fig. 10, this receiver is up to 4 dB better than the receiver without integrated tracking and in-

terpolation. In general, the greater the Doppler change over a data packet, the greater the gain. However, a few packets begin and end with similar Doppler shift so that the Doppler change from start to end is very small. In these cases the performance improvement is a function of the maximum variation, and thus may be small.

The receiver with integrated interpolation that does not use the initial Doppler estimate also offers a significant performance improvement as the Doppler change increases, but suffers a slight loss in MSE with respect to the fixed interpolation rate receiver when the Doppler change is small. The MSE loss, which averages less than one-half dB, is due to the higher PLL gain necessary to acquire and track the carrier phase shift, and the additional noise that this introduces.

D. 4000 sps at 15 kHz Carrier, BPSK

The final case is used to demonstrate that the equalizer with integrated Doppler tracking allows the source and receiver to move such that the relative Doppler shift may change sign within a single data packet. The signal used for the test is 4000 sps BPSK transmitted at a 15 kHz carrier with a duration of 60 s (250 000 symbols). The source used for the test is rigidly mounted below a small boat and it transmits to a fixed, multi-channel receiver. The small boat turned in tight circles a few hundred meters from the receiver as shown in Fig. 11. One and a half revolutions of a 25 m circle were performed at a speed of 2 m/s.

At $t = 0$ the source is starting a turn toward the receiver at a speed of 0.7 m/s. The receiver acquires the Doppler shift during the training period without use of an external estimate. As the turn progresses the relative speed increases to a maximum at $t = 10$ s, then decreases until the sign of the Doppler shift changes at $t = 20$ s. The interpolation filters automatically switch from time-expansion to time-compression as the source goes from closing range to opening. Another sign change occurs at $t = 40$ s as the transmitter turns toward the receiver again.

Throughout the 60 s long packet the PLL maintains lock on the carrier phase that is used to update the time-scale measurement for the interpolator. The conventional receiver without integrated interpolation fails soon after the packet starts because of the changing Doppler shift. This test demonstrates that the receiver can operate continuously through a wide range of Doppler shifts without the need for additional training or other overhead within the data packet.

VI. Conclusion

Time-varying Doppler shift caused by changes in relative source-receiver motion creates both a carrier phase offset and a sample-rate error that degrades the performance of a phase-coherent acoustic communications receiver. The phase-locked loop operated in conjunction with a DFE provides a frequency offset estimate which may be used to compute and correct the instantaneous sample-rate error and cumulative delay. Only a few extra computations per symbol are required. While a few non-demanding applications with little motion may need only the PLL, forcing the adaptive equalizer to perform the time-scale correction inevitably reduces receiver performance.

The fractionally-spaced equalizer typically used for undersea applications limits the required frequency response of an interpolation filter to less than full bandwidth. Taking advantage of this fact leads to a frequency-weighted filter design which may be solved by minimizing the band-limited mean-square error. The least-squares optimal interpolation filter is set for a particular constellation density by adjusting the filter length and its update rate. The BPSK and QPSK signals, which are most commonly used for undersea acoustic communication, require filters of only 3 baseband points with filter updates only every 50 samples. A small filter look-up table and a companion difference table used for filter interpolation minimize the number of computations necessary to generate an interpolation filter.

The method works well for both fast, constant Doppler (straight-line ship motion), or time-varying Doppler (turning vehicles or vertical wave motion). Acquisition performance at speeds faster than several meters per second may be improved by use of an initial Doppler estimate obtained by any number of methods including those described in [6] and [12]. The result is a scalable approach to Doppler compensation suitable for a wide range of data rates and nearly arbitrary platform motion, all without any changes in the transmitted signal.

REFERENCES

[1] G. Ungerboeck, "Adaptive maximum likelihood receiver for carrier modulated data transmission system," *IEEE Tr. Comm*, vol. 22, pp. 624-634, 1974.

[2] S. Prasad and S. Pathak, "On jointly adaptive decision feedback equalization and carrier recovery in digital communication systems," AEÜ, vol. 43, pp. 135-143, 1989.

[3] D. Falconer, "Jointly adaptive equalization and carrier recovery in two dimensional digital communication systems," *Bell Syst. Tech. J.*, vol. 55, pp. 317-334, Mar. 1976.

[4] M. Stojanovic, J. Catipovic and J. Proakis, "Phase coherent digital communications for underwater acoustic channels", *IEEE J. Oceanic Eng.*, Vol. OE-16, pp. 100-111, Jan. 1994.

[5] M. Stojanovic, J. Catipovic and J. Proakis, "Adaptive multi-channel combining and equalization for underwater acoustic communications", *J. Acoust. Soc. Am.*, **94**, (3), part 1, pp. 1621-1631.

[6] M. Johnson, L. Freitag and M. Stojanovic, "Improved Doppler tracking and correction for underwater acoustic communication," *Proc. ICASSP '97*, vol 1, pp. 575-578, Munich, Germany, April, 1997.

[7] L. Freitag, M. Johnson and M. Stojanovic, "Efficient equalizer update algorithms for acoustic communication channels of varying complexity," *Proc. Oceans '97*, pp. 580-585, Oct. 1997.

[8] G. Oetken, T. Parks and H. Schüssler,"New results in the design of digital interpolators," *IEEE Tr. ASSP*, vol. 23, No. 3, June 1976, pp. 301-309.

[9] D. Kim, M. J. Narasimha and D. C. Cox, "Design of optimal interpolation filter for symbol timing recovery," *IEEE Tr. Comm.*, vol. 45, No. 7, July 1997, pp. 877-884.

[10] F. M. Gardner, "Interpolation in digital modems–part I: fundamentals," *IEEE Tr. Comm.*, vol. 41, No. 3, March 1993, pp. 501-507.

[11] L. Erup, F. M. Gardner and R. Harris, "Interpolation in digital modems–part II: implementation and performance." *IEEE Tr. Comm.*, vol. 41, No. 6, June 1993, pp. 998-1008.

[12] B. S. Sharif, J. Neasham, O. R. Hinton and A. E. Adams,"A computationally efficient Doppler compensation system for underwater acoustic communication," *IEEE J. Oceanic Eng.*, Vol. OE-25, pp. 52-61, Jan. 2000.

[13] I. Schumacher and G. J. Heard, "Removal of time-varying Doppler using phase tracking with application to ocean warming measurements," *J. Acoust. Soc. Am.*, **96** (3), Sept. 1994, pp. 1805-1812.

[14] L. Brekhovskikh and Y. Lysanov, *Fundamentals of Ocean Acoustics*, New York: Springer, 1982.

[15] T. Rappaport, *Wireless Communications: Principles and Practice*, Upper Saddle River, NJ: Prentice Hall, 1996.

[16] L. Freitag, M. Johnson, M. Stojanovic, D. Nagle and J. Catipovic, "Survey and analysis of underwater acoustic channels for coherent communication in the medium-frequency band," *Proc. Oceans 2000*, Providence, Sept. 2000.

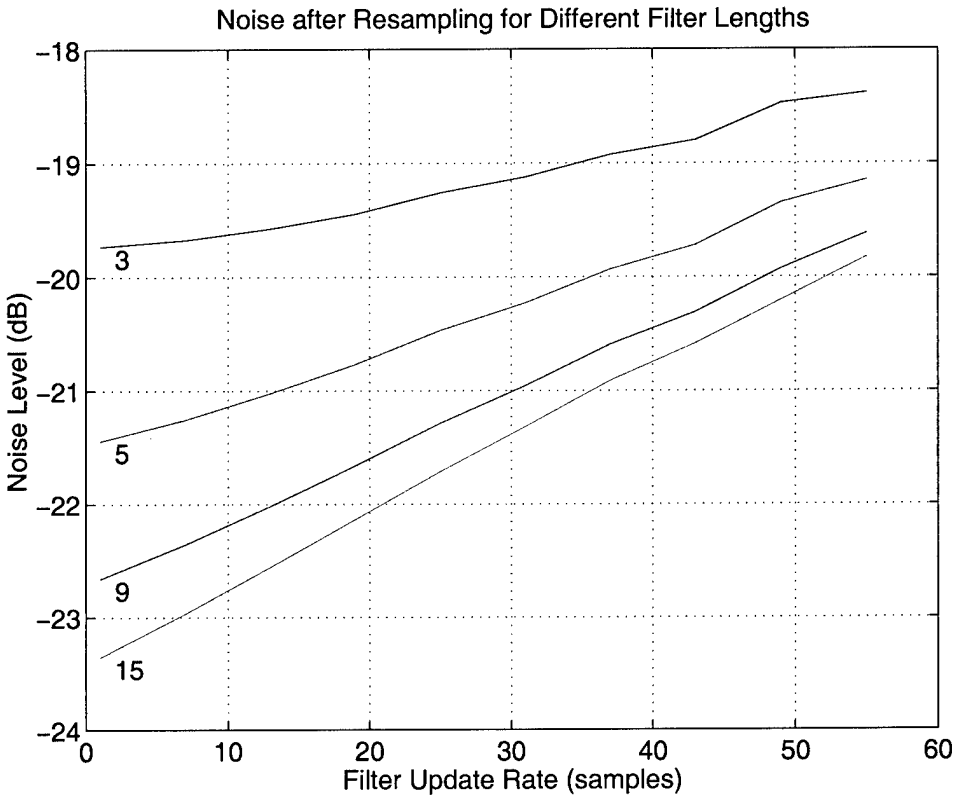

Fig. 1. Interpolation filter performance for $\omega_o = pi/2$ at time-scale factor 1.0025.

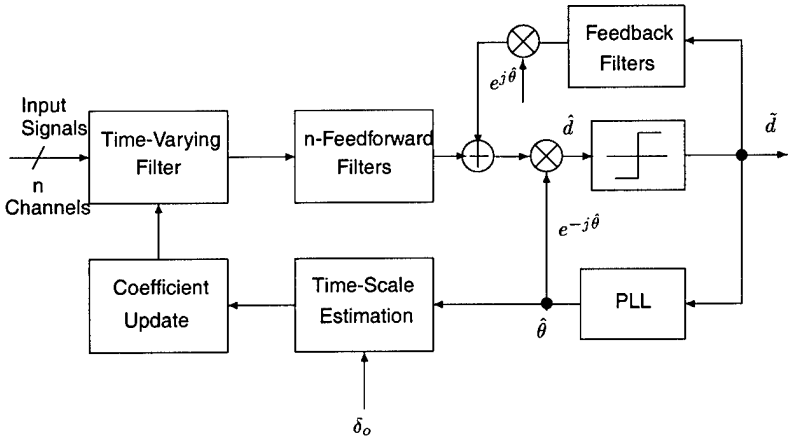

Fig. 2. Receiver block diagram.

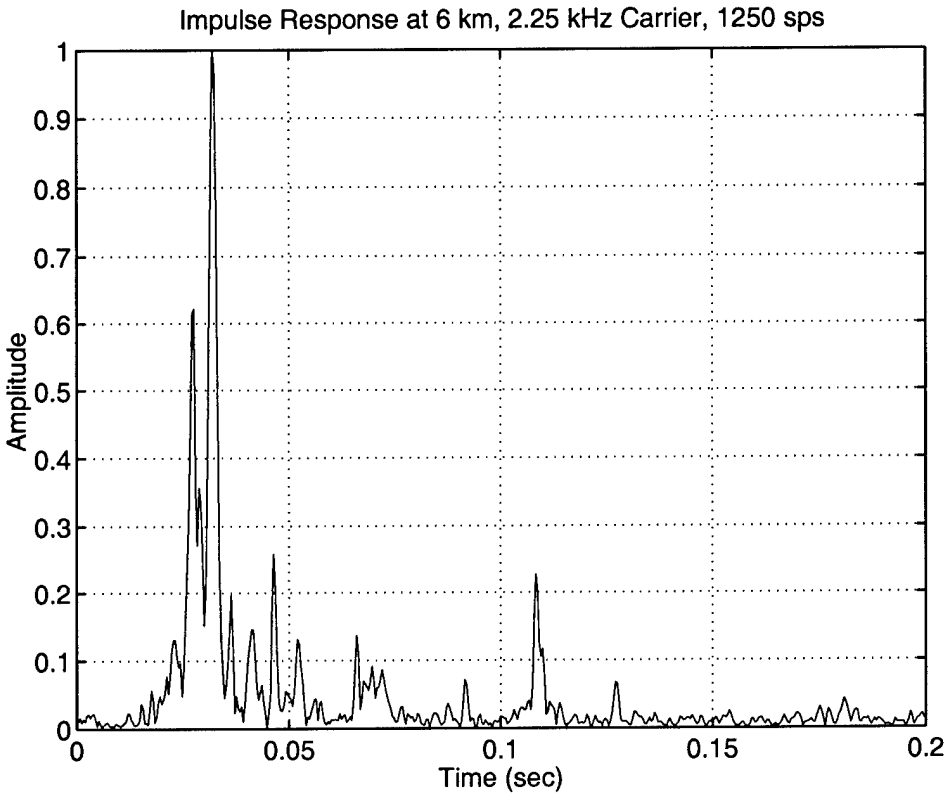

Fig. 3. Impulse Response for Case A.

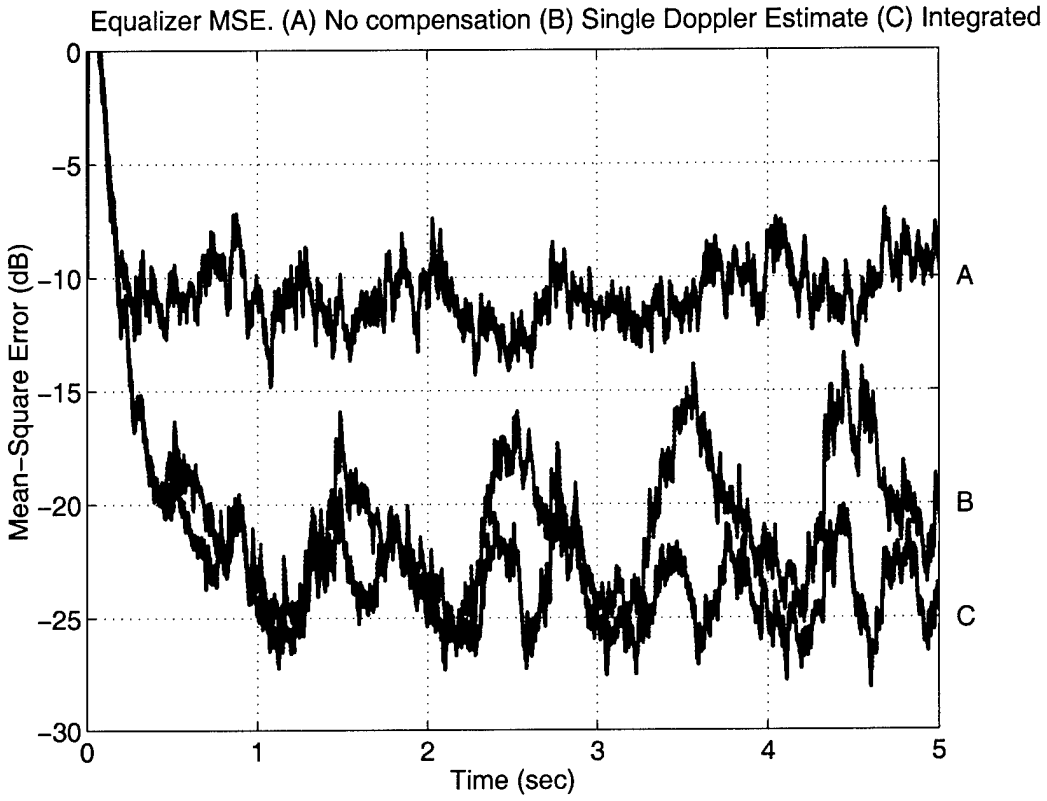

Fig. 4. Equalizer MSE for Case A processed three different ways. (A) No interpolation to correct the time-scale. (B) Interpolation based on a Doppler estimate obtained at the start of the packet. (C) Continuously estimated and compensated.

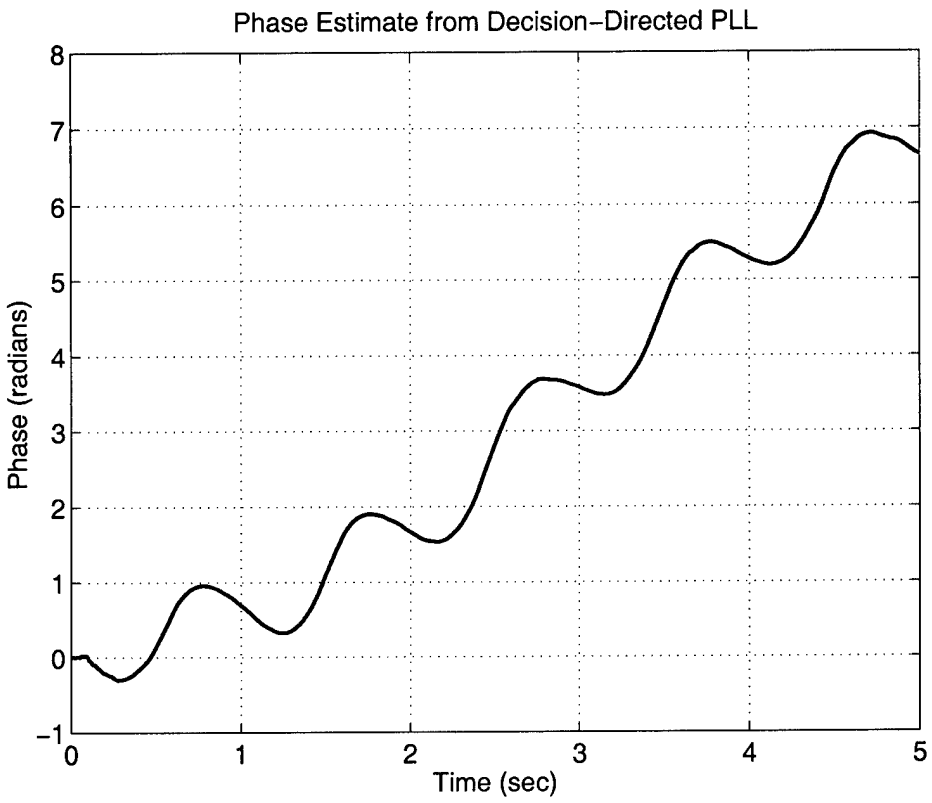

Fig. 5. Phase estimated by the PLL for Case A.

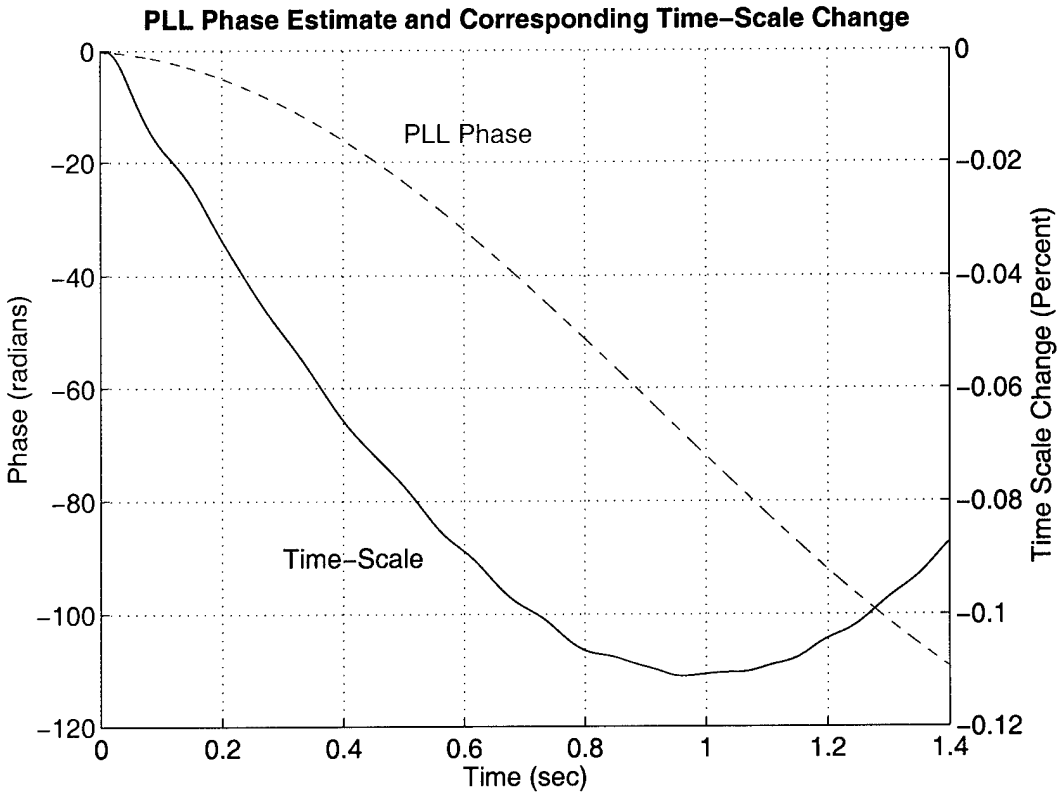

Fig. 6. Vertical channel phase and time-scale change due to surface heave for Case B.

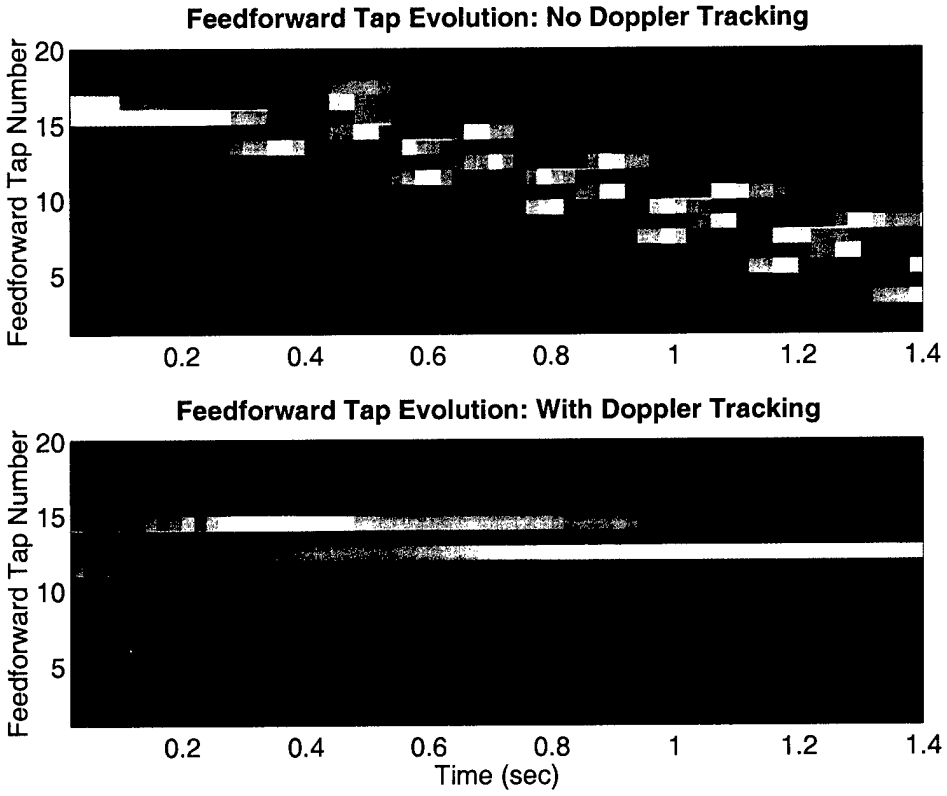

Fig. 7. Feedforward tap magnitude for vertical channel communications without integrated Doppler tracking and resampling (top), and with integrated processing (bottom).

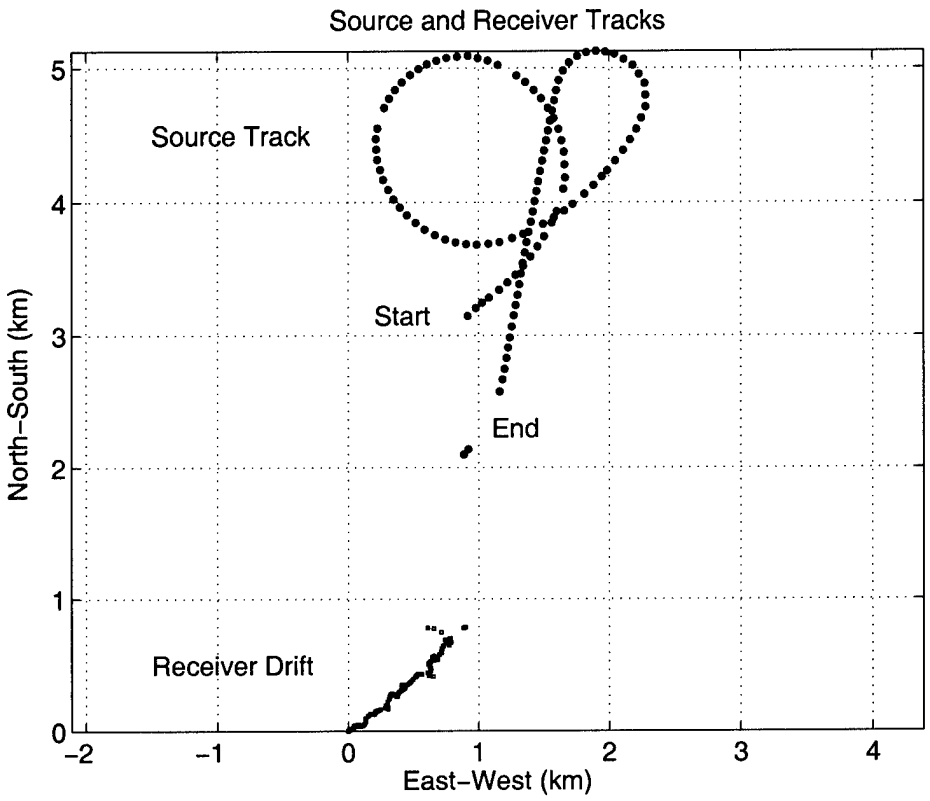

Fig. 8. Source-receiver test tracks for Case C.

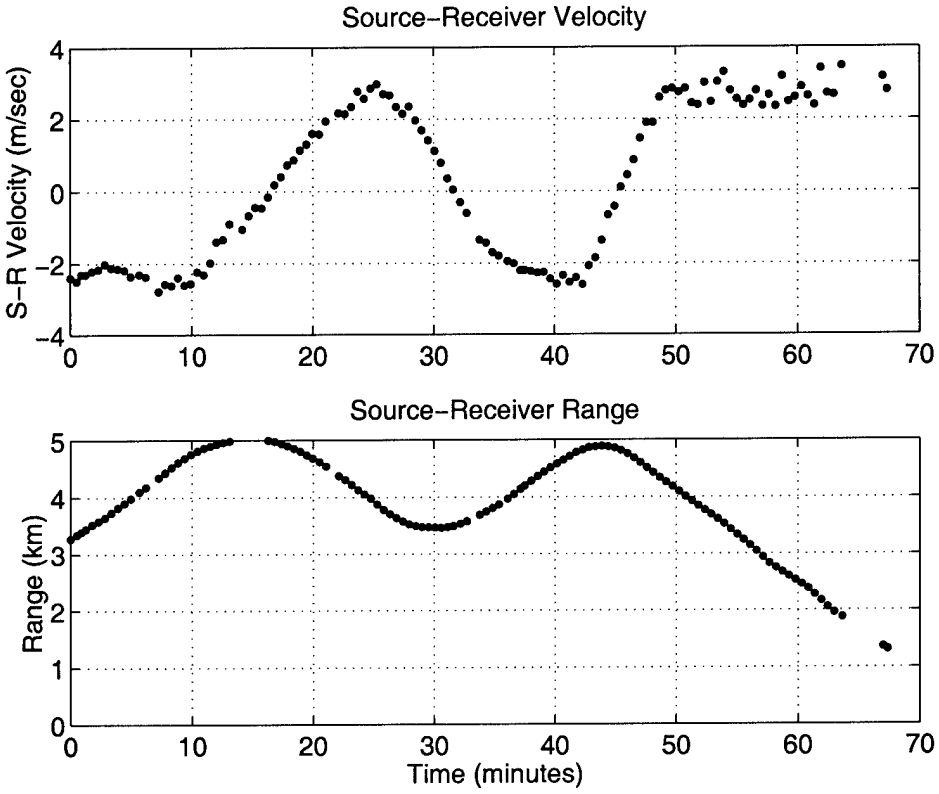

Fig. 9. Velocity and range between source and receiver for Case C.

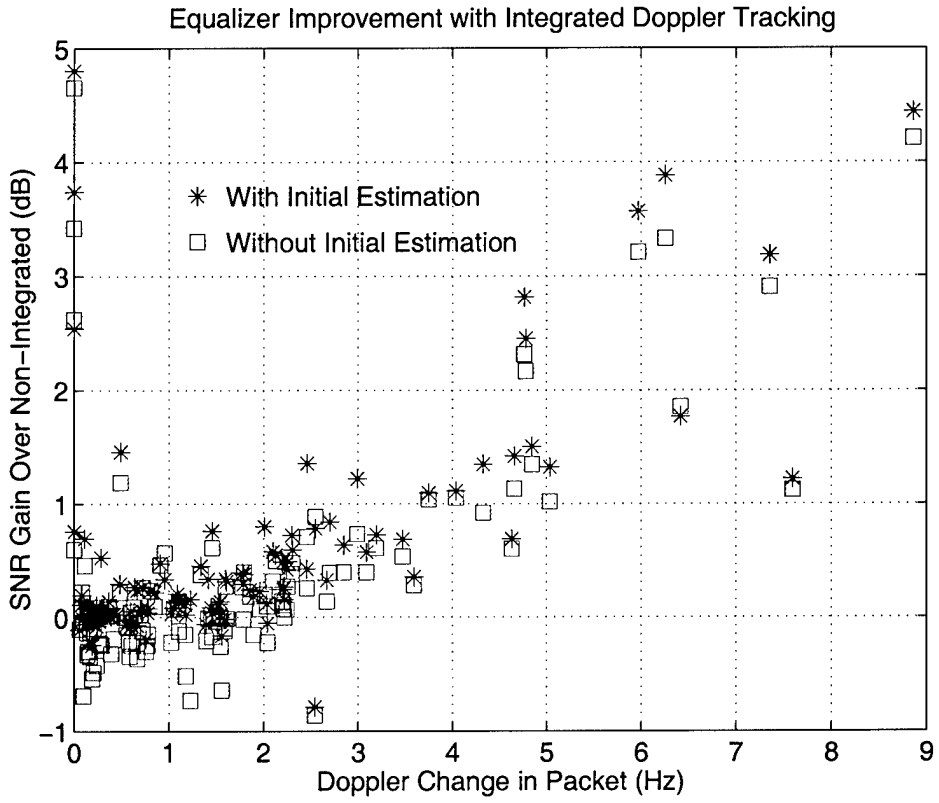

Fig. 10. Improvement of the Doppler tracking receiver with respect to the receiver with initial Doppler estimation and fixed resampling rate (case C).

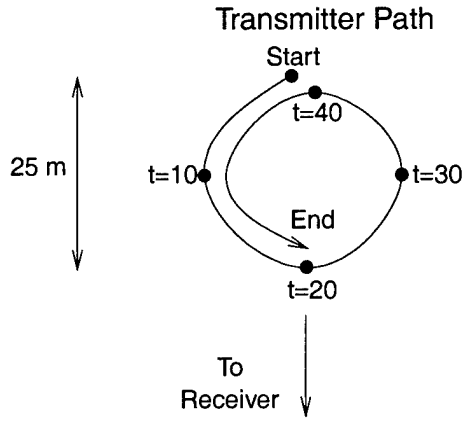

Fig. 11. Path of small boat while transmiting a 60 s continuous signal for Doppler change test (Case D).

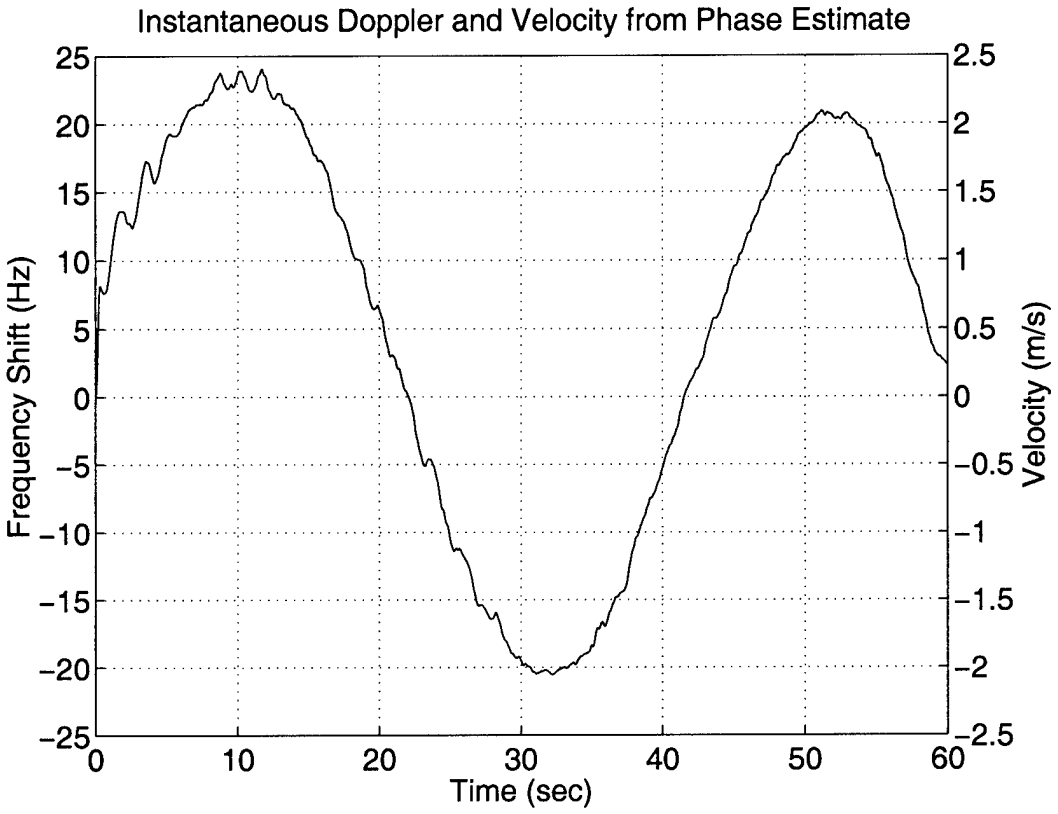

Fig. 12. Doppler frequency shift and resulting relative source-receiver velocity while the source follows the track in Fig. 11.

Project **13035700** **Woods Hole Oceanographic Institution** Project **13035700**

Investigator **FREITAG, LEE E** Funding Agency **ONR-GRANTS**
Duration **03/01/2000-09/30/2001 INACTIVE** Agency Program **ONR - OTHER**

Project Ledger Report
13035700 HIGH-DOPPLER COMMUNICATIONS
For the period ending July 17, 2002

Acct.	Account Name	Budget	Current Activity	Year To Date Activity	Inception To Date Activity	Encumb.	Available Balance	Pcnt Expd.
5010	Salaries - Regular	73,255.00	0.00	0.00	65,835.61	0.00	7,419.39	89
5015	Salaries-Casual	0.00	0.00	0.00	562.51	0.00	(562.51)	
5040	Salaries - Overtime	0.00	0.00	0.00	130.31	0.00	(130.31)	
5050	Fringe Benefits Regular	25,537.00	0.00	0.00	23,063.60	0.00	2,473.40	90
5052	Fringe Benefits Overtime	0.00	0.00	0.00	10.33	0.00	(10.33)	
5054	Fringe Benefits-Casual	0.00	0.00	0.00	40.44	0.00	(40.44)	
5060	Lab Costs Regular	44,071.00	0.00	0.00	40,282.44	0.00	3,788.56	91
5062	Lab Costs Overtime App	0.00	0.00	0.00	43.36	0.00	(43.36)	
5066	Laboratory Costs - Casual	0.00	0.00	0.00	268.98	0.00	(268.98)	
5100	Elec/Mech/Carp. shop services	680.00	0.00	0.00	2,856.89	0.00	(2,176.89)	420
5130	Graphics shop services	624.00	0.00	0.00	0.00	0.00	624.00	0
5170	Travel - Domestic	5,369.00	0.00	0.00	275.57	0.00	5,093.43	5
5210	Supplies	2,400.00	0.00	0.00	10,986.14	0.00	(8,586.14)	457
5212	Computer Supplies	0.00	0.00	0.00	3,248.38	0.00	(3,248.38)	
5220	Books & Publications	0.00	0.00	0.00	92.00	0.00	(92.00)	
5230	Safety Wear	0.00	0.00	0.00	97.00	0.00	(97.00)	
5250	Stockroom Supplies	600.00	0.00	0.00	371.37	0.00	228.63	61
5310	Other Outside Services	0.00	0.00	0.00	4,100.00	0.00	(4,100.00)	
5332	Equipment Maintenance Agreemnt	1,200.00	0.00	0.00	0.00	0.00	1,200.00	0
5360	Communications	900.00	0.00	0.00	116.89	0.00	783.11	12
5370	Shipping & Postage	500.00	0.00	0.00	145.45	0.00	354.55	29
5410	Miscellaneous	0.00	0.00	0.00	739.47	0.00	(739.47)	
5430	Duplicating	492.00	0.00	0.00	2.89	0.00	489.11	0
5510	Technical Assistance	0.00	0.00	0.00	22.44	0.00	(22.44)	
5600	Ship Use	7,750.00	0.00	0.00	620.00	0.00	7,130.00	8
5601	Asterias	0.00	0.00	0.00	0.00	0.00	0.00	
5690	Small Boats Use	0.00	0.00	0.00	1,617.89	0.00	(1,617.89)	
5870	Refunds & Adjustments	(13,644.76)	0.00	0.00	(1,079.05)	0.00	(12,565.71)	7
5960	G & A Regular	36,622.00	0.00	0.00	31,644.79	0.00	4,977.21	86
5962	G & A Overtime App	0.00	0.00	0.00	36.03	0.00	(36.03)	
5966	G&A Overhead-Casual	0.00	0.00	0.00	223.51	0.00	(223.51)	
	Total Costs	**186,355.24**	**0.00**	**0.00**	**186,355.24**	**0.00**	**(-0.00)**	**100 %**
	Salaries and Fringe Benefits	**98,792.00**	**0.00**	**0.00**	**89,642.80**	**0.00**	**9,149.20**	**90 %**
	Laboratory Costs	**44,071.00**	**0.00**	**0.00**	**40,594.78**	**0.00**	**3,476.22**	**92 %**
	General and Administrative	**36,622.00**	**0.00**	**0.00**	**31,904.33**	**0.00**	**4,717.67**	**87 %**
	Other Costs	**6,870.24**	**0.00**	**0.00**	**24,213.33**	**0.00**	**(-17,343.09)**	**352 %**

Created: **Jul 17, 2002** **04 - APPLIED OCEAN PHYSICS-ENGINEER** Grant **Unknown**

Last revision 07/04/00 04:36 PM

Subject: [Fwd: Revised no-cost extension request for N000140010357]
Date: Wed, 17 Jul 2002 11:33:17 -0400
From: Lee Freitag <lfreitag@whoi.edu>
Organization: Woods Hole Oceanographic Institution
To: Dolores Chausse <dchausse@whoi.edu>

--
Lee Freitag, Senior Engineer
Mail Stop 18
Woods Hole Oceanographic Institution
Woods Hole, MA 02543
508.289.3285
508.457.2195 (fax)

Subject: Revised no-cost extension request for N000140010357
Date: Thu, 21 Dec 2000 15:47:55 -0500
From: Lee Freitag <lfreitag@whoi.edu>
Organization: Woods Hole Oceanographic Institution
To: "Jacobi, Les" <jacobil@ONR.NAVY.MIL>
CC: "Comer, G. Kevin" <COMERG@ONR.NAVY.MIL> ,
"Cady, Claire" <Claire_Cady@onr.navy.mil> ,
"Rideout, Darlene" <RIDEOUD@ONR.NAVY.MIL> ,
Tom Nemmers <tnemmers@whoi.edu> , Sue Ferreira <suferreira@whoi.edu>

Les,

Thanks for the quick reply. Here is the revised request for extension.

We would like to request an extension to May. 31, 2001 for the program "Acoustic Communication for High-Doppler Guidance and Control", that is currently due to expire Feb. 28, 2001.

The extension is needed due to delays in performing the data collection experiments at NUWC, Newport and in getting the full set of raw data from those tests. The extension to 5/31/01 will allow complete analysis of the data and completion of reports and papers.

As of 12/20/2000 the amount of funds remaining is $122,664.85.

Thank you very much for your support and please don't hesitate to contact me if you have any questions.

Regards,

Lee

Lee Freitag, Senior Engineer
Mail Stop 18
Woods Hole Oceanographic Institution
Woods Hole, MA 02543
508.289.3285
508.457.2195 (fax)